1

Ultracold atoms in optical lattices

In this chapter we introduce the reader to the physics of ultracold atoms trapped in crystals made of light: optical lattices. The chapter begins with a review of the foundations of atom-light interactions and explains how those interactions can be used to trap and manipulate atoms. Then it takes a route through the basic physics describing the behavior of cold atoms trapped in optical lattices. It starts with the simple noninteracting regime, where important concepts such as band structure, Bloch waves and Wannier functions are introduced, and then goes into the the strongly interacting regime where new states of matter such as the so called Mott insulator state emerge. The chapter discusses standard theoretical methods commonly used to deal with interacting systems and apply them to calculate the phase diagram of the Bose Hubbard model which describes bosonic atoms hopping in a lattice and interacting only when more than two occupy the same lattice site. In the following chapter we will use the techniques introduced here to compute quantum correlations and other many body properties.

1.1 Optical lattices

Optical lattices are artificial crystals of light created by interfering optical laser beams. When atoms are illuminated with laser beams, the electric field of the laser induces a dipole moment in the atoms which in turn interacts with the electric field. This interaction modifies the energy of the internal states of the atoms in a way that depends both on the light intensity and on the laser frequency. A spatially dependent intensity induces a spatially dependent potential energy which can be used to trap the atoms. An optical lattice is the periodic potential energy landscape that the atoms experience as a result of the standing wave pattern generated by the interference of laser beams.

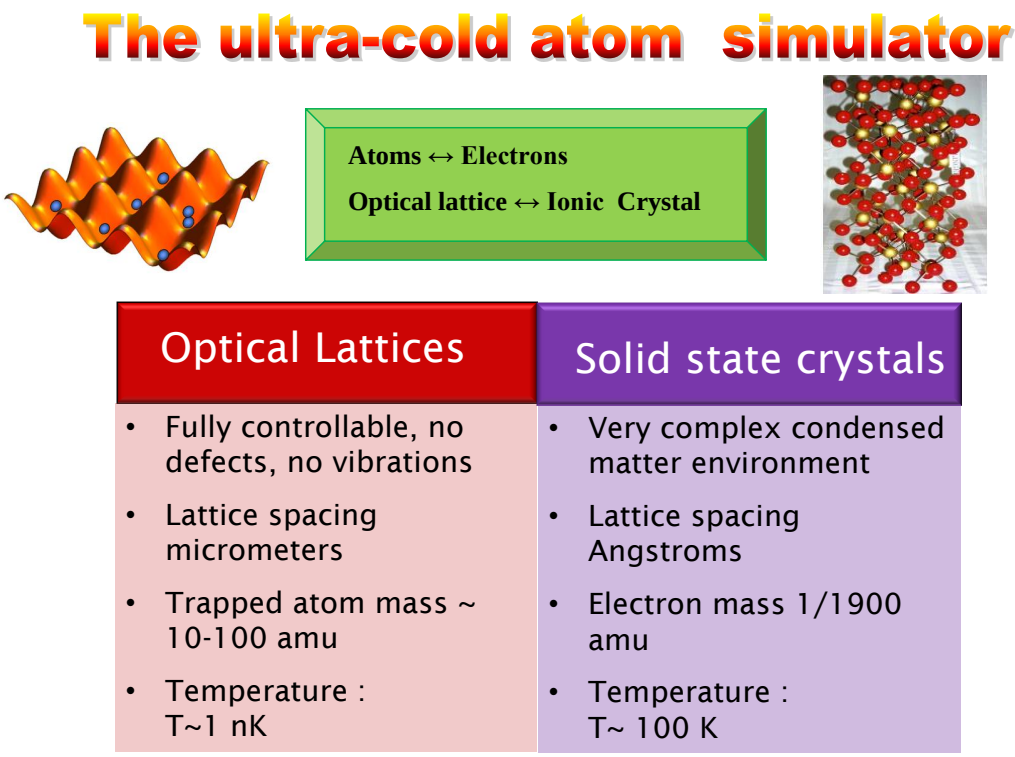

Figure 1.1 Optical lattice vs solid state crystal lattices. Atoms trapped in optical lattices can be used to mimic the behavior of conduction electrons in solid state crystals.

Optical lattices have been widely used in atomic physics as a way to cool, trap and control atoms. In the recent years ultracold atoms in optical lattices have become a unique meeting ground for simulating solid state materials [Bloch et al. (2008)]. The optical lattice potential mimics the crystal lattice in a solid and the atoms loaded in the lattice mimic the valence electrons (See figure 1.2). Atoms move in the lattice (actually tunnel quantum-mechanically between lattice sites) as valence electrons do in the periodic energy landscape generated by the positively charged ions in a solid crystal.

There are, however, some important difference between solid-state crystals and optical lattice which are relevant to emphasize. First of all the energy scales in consideration are very different. While the typical lattice spacing in cold atoms systems is of the order of one μm, in solid-state crystals it is around 0.1 nm. Atoms are also much heavier than electrons. That means that to probe the same physics that occurs at 100 kelvin temperatures in solid-

state systems we need to cool to atoms below a few nanokelvin. The much lower energy scale requires the need of state-of-the-art cooling techniques but is advantageous for probing. Ultra-cold atomic systems do not require sophisticated ultra-fast probes. In such systems it is possible to follow the dynamics of the atoms on the time scales of ms or even seconds. Moreover, in contrast to electrons which are charged particles and strongly coupled to the complex solid-state environment, atoms are neutral and almost completely decoupled from their environment. In contrast to real materials where disorder, lattice vibrations and structural defects are inevitable, crystals made by light are rigid (no vibrations), free of defects and fully controllable.

The lattice geometry is determined by the configuration of laser beams used to create the lattice and the lattice depth is tunable by the laser intensity. There is even flexibility in controlling the lattice spacing by modifying the interference angle between the laser beams. By controlling the intensity of the trapping laser beams the dimensionality of the system can be varied from 3D to 0D even dynamically during the course of an experiment. Thanks to all these attributes ultra-cold atoms loaded in optical lattice have become a perfect arena for the investigation of non-linear phenomena, quantum phase transitions and non-equilibrium dynamics. Atoms loaded in optical lattices have also been proposed as ideal quantum information processors.

1.1.1 Basic Theory of optical lattices

Let us first start by explaining in more detail how optical lattice potentials are generated. Neutral atoms interact with light in both *dissipative* and *conservative* ways. The conservative interaction comes from the interaction of the light field with the induced dipole moment of the atom which causes a shift in the potential energy called **AC-Stark shift**. The dissipative interaction comes due to the absorption of photons followed by spontaneous emission. Laser cooling techniques make use of this dissipative process [Phillips (1998)]. In this chapter we will mainly concentrate on the conservative part of the interaction and just briefly mention the the basic origin and consequences of the dissipative part.

AC Stark Shift

Consider a two level atom, with internal ground state $|g\rangle$ and excited state $|e\rangle$ separated by an energy $\hbar\omega_0$. The atom is illuminated with a classical electromagnetic field $\boldsymbol{E} = \boldsymbol{\mathcal{E}}(\mathbf{x})e^{-\mathrm{i}\omega t} + \boldsymbol{\mathcal{E}}^*(\mathbf{x})e^{\mathrm{i}\omega t}$ with amplitude $\mathcal{E}(\mathbf{x})$ and angular frequency $\omega = 2\pi\nu$ as schematically shown in Fig.1.2.

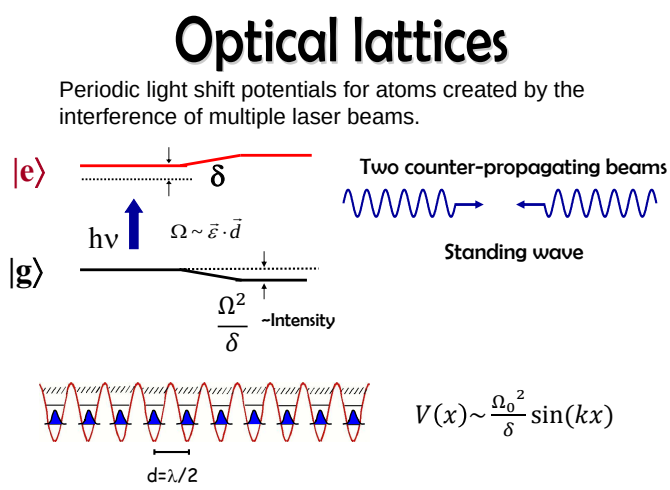

Figure 1.2 AC Stark shift induced by atom-light interaction. The laser frequency is $\omega = 2\pi\nu$ which is detuned from the atomic resonance by δ

The electromagnetic field induces a dipole moment in the atom, $\hat{\mathbf{d}}$, which interacts with it in the usual way:

$$V = -\hat{\boldsymbol{d}} \cdot \boldsymbol{E} \tag{1.1}$$

Quantum mechanically the dipole moment is an operator and can be written in the two level atom basis as: $\hat{\boldsymbol{d}} = \sum_{\alpha,\beta=e,g} \langle\alpha|\hat{\boldsymbol{d}}|\beta\rangle|\alpha\rangle\langle\beta|$. Note that $\sum_\alpha |\alpha\rangle\langle\alpha| = 1$. Since atoms do not have a permanent dipole moment, $\langle\alpha|\hat{\boldsymbol{d}}|\alpha\rangle = 0$, and only the off-diagonal terms are non-zero $\boldsymbol{\mu}_{eg} = \langle e|\hat{\boldsymbol{d}}|g\rangle \neq 0$. Those determine the induced dipole moment. This means that $\hat{d} = \boldsymbol{\mu}_{eg}|e\rangle\langle g| + \boldsymbol{\mu}^*_{eg}|g\rangle\langle e|$, and the total Hamiltonian of the system can be written as:

$$\hat{H} = \hbar\omega_0 |e\rangle\langle e| - \left(\boldsymbol{\mu}_{eg}|e\rangle\langle g| + \boldsymbol{\mu}^*_{eg}|g\rangle\langle e|\right) \cdot \left(\boldsymbol{\mathcal{E}}(\mathbf{x})e^{-\mathrm{i}\omega t} + \boldsymbol{\mathcal{E}}^*(\mathbf{x})e^{\mathrm{i}\omega t}\right), \tag{1.2}$$

When the laser detuning $\delta = \omega - \omega_0$ is small, $|\delta| \ll |\omega - \omega_0|$, a convenient way to proceed is to make the Hamiltonian time independent by going to the rotating frame of the laser. The Hamiltonian in this rotating frame, determined by the unitary transformation $\hat{U}(t) = e^{-\mathrm{i}\omega t\hat{\sigma}_z/2}$ with $\hat{\sigma}_z = |e\rangle\langle e| - |g\rangle\langle g|$ the corresponding Pauli matrix in the e, g basis, transforms to $\hat{H} \to \hat{U}^\dagger\hat{H}\hat{U} + \mathrm{i}\hbar\frac{\partial\hat{U}^\dagger}{\partial t}\hat{U}$. After neglecting processes with a rapidly oscillating phase, $\exp(-i(\omega_0 + \omega)t)$ which average out over time, the Hamiltonian becomes

$$\hat{H} = -\frac{\hbar\delta}{2}\hat{\sigma}_z - \left(\frac{\hbar\Omega(\vec{x})}{2}\left|e\right\rangle\left\langle g\right| + \frac{\hbar\Omega^*(\vec{x})}{2}\left|e\right\rangle\left\langle g\right|\right), \tag{1.3}$$

where $\Omega(\mathbf{x})$ is the so called Rabi frequency given by $\hbar\Omega(\mathbf{x}) = 2\boldsymbol{\mathcal{E}}(\mathbf{x})\cdot\boldsymbol{\mu}_{ge}$.

If the detuning is large compared to the Rabi frequency, $|\delta| \gg \Omega$, the effect of the atom-light interactions on the states $|e\rangle$ and $|g\rangle$ can be determined with second order perturbation theory. In this case, the energy shift $E^{(2)}_{g,e}$ is given by

$$E^{(2)}_{g,e} = \pm\frac{|\left\langle e\right|\hat{H}\left|g\right\rangle|^2}{\hbar\delta} = \pm\hbar\frac{\Omega(\mathbf{x})^2}{4\delta}, \tag{1.4}$$

with the plus and minus sign for the $|g\rangle$ and $|e\rangle$ states respectively. This energy shift, $\hbar\frac{\Omega(\mathbf{x})^2}{4\delta}$ is the so called ac-Stark shift and defines the optical potential that atoms in the state $|g\rangle$ experience the g atoms feel due to their interaction with light. If instead of interacting with an single electromagnetic field, the atoms are illuminated with superimposed counter propagating laser beams which interfere, the atoms will feel the standing wave pattern resulting from the interference. This periodic landscape modulation of the energy experienced by the atoms is the so-called optical lattice potential.

In the above discussion we implicitly assumed that the excited state has an infinite life time. However, in reality it will decay by spontaneous emission of photons. This effect can be taken into account phenomenologically by attributing to the excited state an energy with both real and imaginary parts. If the excited state has a life time $1/\Gamma_e$, the energy of the perturbed ground state becomes a complex quantity which we can write as

$$E^{(2)}_g = \frac{\hbar}{4}\frac{\Omega(\mathbf{x})^2}{\delta - i\Gamma_e/2} = V(\mathbf{x}) + i\gamma_{sc}(\mathbf{x}), \tag{1.5}$$

$$V(\mathbf{x}) = \hbar\frac{\Omega(\mathbf{x})^2\delta}{4\delta^2 - \Gamma_e^2} \approx \hbar\frac{\Omega(\mathbf{x})^2}{4\delta}, \quad \gamma_{sc}(\mathbf{x}) = \frac{\hbar}{2}\frac{\Omega(\mathbf{x})^2\Gamma_e}{4\delta^2 - \Gamma_e^2} \approx \hbar\frac{\Omega(\mathbf{x})^2\Gamma_e}{8\delta^2}. \tag{1.6}$$

The real part of the energy corresponds to the optical potential $V(\mathbf{x})$. The sign of the optical potential seen by the atoms depend on the sign of the detuning. For blue detuning , $\delta > 0$, the sign is positive resulting in a repulsive potential. The potential minima corresponds to the points with zero light intensity. Atoms are repealed from the high intensity regions. On the other hand, in a red detuned light field, $\delta < 0$, the potential is attractive, the minima correspond to the places with maximum light intensity where atoms want to stay at. One will often find in the literature the description of atoms as "weak field seekers" or "strong field seekers" for cases of blue and red detuning, respectively. The imaginary part, $\gamma_{sc}(\mathbf{x})$ represents the the loss

rate of atoms from the ground state. For large detunings the conservative part of the optical potential dominates and can be used to trap the atoms.

Lattice Geometry

The simplest possible lattice is a one dimensional lattice (1D) lattice. It can be generated by creating a standing wave interference pattern by retro reflection of a single laser beam with Rabi frequency Ω_0. This results in a Rabi frequency $\Omega(x) = 2\Omega_0 \sin(kx)$ which yields a periodic trapping potential given by

$$V_{lat}(x) = V_0 \sin^2(kx) = \frac{\hbar\Omega_0^2}{\delta} \sin^2(kx) \tag{1.7}$$

where $k = 2\pi/\lambda$ is the magnitude of the laser-light wave vector and V_0 is the lattice depth. This potential has a lattice constant, a, defined by the condition $V_{lat}(x + a) = V_{lat}(x)$ for all x. This lattice constant is $a = \lambda/2$.

Note that mimicking solid state crystals with an optical lattice has the great advantage that, in general, the lattice geometry can be controlled easily by changing the laser fields.

Periodic potentials in higher dimensions can be created by superimposing more laser beams. To create a two dimensional lattice potential for example, two orthogonal sets of counter propagating laser beams can be used. In this case the lattice potential has the form

$$V_{lat}(x, y) = V_o \left(\cos^2(ky) + \cos^2(kx) + 2\varepsilon_1 \cdot \varepsilon_2 \cos\phi \cos(ky)\cos(kx)\right), \tag{1.8}$$

Here k is the wave vector magnitude, ε_1 and ε_2 are polarization vectors of the counter propagating set and ϕ is the phase between them. A simple square lattice can be created by choosing orthogonal polarizations between the standing waves. In this case the interference term vanishes and the resulting potential is just the sum of two superimposed 1D lattice potentials. Even if the polarization of the two pair of beams is the same, they can be made independent by detuning the common frequency of one pair of beams from that the other.

A more general class of two 2D lattices can be created from the interference of three laser beams [Blakie and Porto (2004); Sebby-Strabley et al. (2006); Wirth et al. (2011); Soltan-Panahi et al. (2011); Tarruell et al. (2012); Jo et al. (2012)] which in general yield non-separable lattices. Such lattices can provide better control over the number of nearest neighbors and allow for the exploration of richer physics. In Fig. 1.3 we show a variety of possible 2D optical lattice geometries that can be made by three and four interfering laser beams. Different type of lattice potentials can be created in 3D by the

interference of al least 5 laser beams. The interference of laser beams with two different wavelengths also gives rise to superlattice structures, such as chequerboard lattices, which allow further controllability of the atoms [Bloch et al. (2008)].

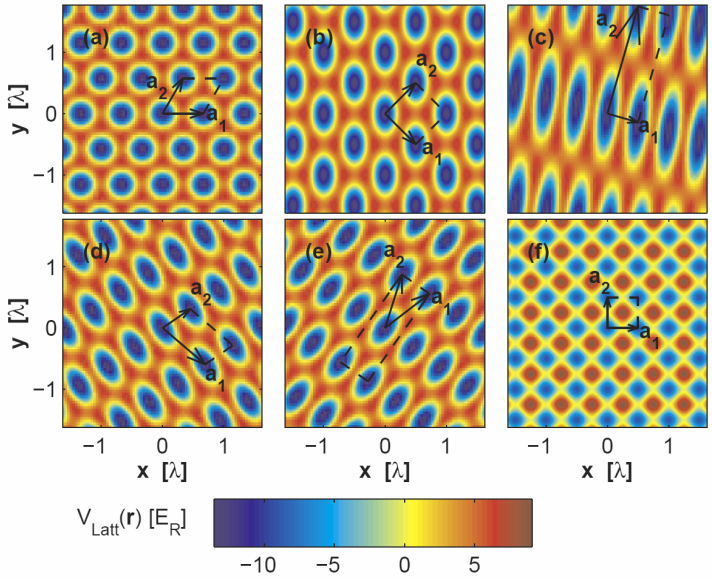

Figure 1.3 Different optical lattice geometries.(a) A hexagonal lattice, (b) A square lattice, (c) A rectangular lattice, (d) An oblique lattice, (e) A centered rectangular lattice, (f) A four beam square lattice. Lattice potentials (a)-(e) are for different configurations of 3 beams, (f) is a potential due to two orthogonal pairs of counter-propagating laser beams. This figure has been taken from Blakie and Porto (2004).

1.2 Single-particle physics

In free space the kinetic energy of an atom is just $p^2/2m$. Here p is the magnitude of the momentum and m the atom mass. An optical lattice potential fundamentally modifies this quadratic dispersion relation. The reason is that in the presence of the lattice, forbidden energy regions appear as a consequence of the diffraction of the quantum mechanical waves in the periodic potential. Those regions give rise to the so called "band structure". One elegant derivation of the band structure uses the so-called Bloch theorem.

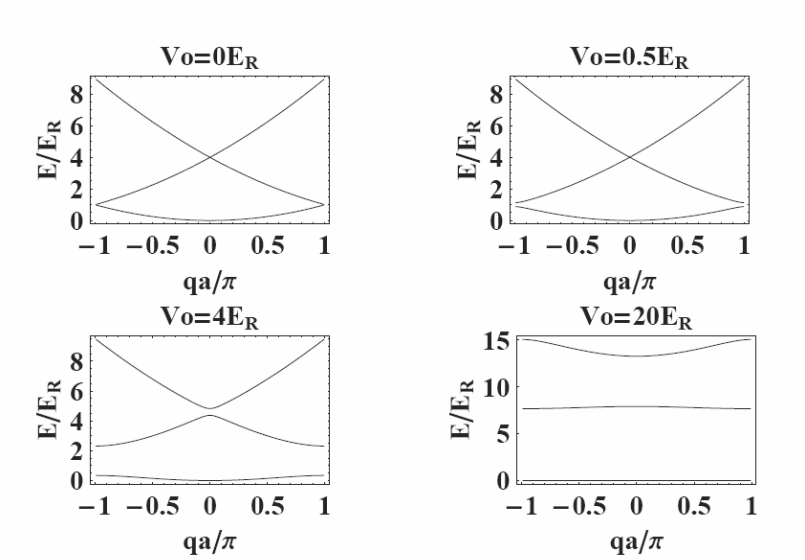

Figure 1.4 Band structure in a periodic potential

1.2.1 Bloch functions

Consider a one-dimensional particle described by the Hamiltonian $H = \frac{\hat{p}^2}{2m} + V_{lat}(x)$, where $V_{lat}(x) = V_{lat}(x+a)$. Bloch's theorem [Ashcroft and Mermin (1976); Ziman (1964)] states that the eigenstates $\phi_q^{(n)}(x)$ can be chosen to have the form of a plane wave times a function with the periodicity of the potential:

$$\phi_q^{(n)}(x) = e^{iqx} u_q^{(n)}(x), \tag{1.9}$$

$$u_q^{(n)}(x+a) = u_q^{(n)}(x). \tag{1.10}$$

Using this ansatz into the Schrödinger equation, $H\phi_q^{(n)}(x) = E_q^{(n)}(x)\phi_q^{(n)}(x)$, yields an equation for $u_q^{(n)}(x)$ given by:

$$\left[\frac{(\hat{p}+\hbar q)^2}{2m} + V_{lat}(x)\right] u_q^{(n)}(x) = E_q^{(n)} u_q^{(n)}(x) \tag{1.11}$$

Note Bloch's theorem introduces a wave vector q. The quantity q should be viewed as a quantum number associated with the translational symmetry of the periodic potential, just as the momentum is a quantum number

associated with the full translational symmetry of free space. It turns out that, in the presence of a periodic potential, $\hbar q$ plays the same fundamental role in the dynamics as does the momentum in free space. To emphasize this similarity $\hbar q$ is called the *quasimomentum* or *crystal momentum* . In general the wave vector q is confined to the first Brilloiun zone, a uniquely defined primitive cell in momentum space. In 1D systems the Brilloiun zone corresponds to $-K/2 < q \leq K/2$. $K = 2\pi/a$ is the so called reciprocal lattice vector.

The index n (band index), appears in Bloch's theorem because for a given q there are many solutions to the Schrödinger equation. Eq. (1.11) can be seen as a set of eigenvalue problems: one eigenvalue problem for each q, each one characterized by an infinite family of solutions with a discrete spectrum labeled by n. On the other hand, because the wave vector q appears only as a parameter in Eq. (1.11), the energy levels for a fixed n has to vary continuously as q varies. The description of energy levels in a periodic potential in terms of a family of continuous functions $E_q^{(n)}$ each with the periodicity of a reciprocal lattice vector, $K = 2\pi/a$, is referred as the band structure. The lattice potential is generally expressed in units of the atom recoil energy, $E_R = \hbar^2 k^2/(2m)$, with $k = \pi/a$. Fig. 1.4 shows the band structure of a sinusoidal potential. For $V_0 = 0$, the atoms are free and the spectrum is quadratic in q. For a finite lattice depth, a bands structure appears. The band gap increases and the band width decreases with increasing lattice depth.

1.2.2 Wannier orbitals

In the absence of a lattice the eigenfunctions of the free system are plane waves. In the presence of an optical lattice plane waves map into Bloch functions. Bloch functions are fully delocalized but, their weight around the potential minima increases with lattice depth (see Fig. 1.5).

Wannier orbitals, a set of orthonormalized wave functions that fully describe particles in a band and which are maximally localized at the lattice sites, form an alternative basis which will be shown to be useful to describe the dynamics of interacting atoms in a lattice. They are defined as:

$$w_n(x - x_i) = \frac{1}{\sqrt{L}} \sum_q e^{-iqx_i} \phi_q^{(n)}(x), \tag{1.12}$$

where the sum runs over q's in the first Brillouin zone, L is the total number

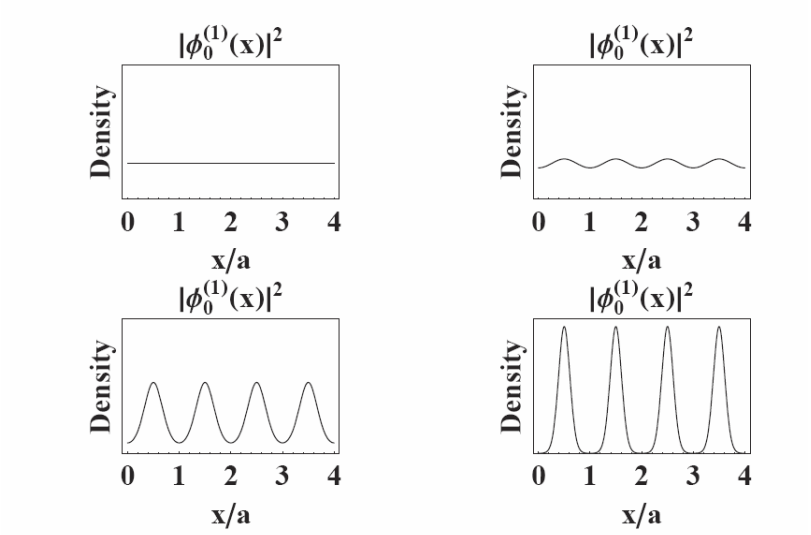

Figure 1.5 Bloch functions in a periodic potential. Similar lattice depths than those ones of Fig.1.4

of lattice sites and x_i is the position of the i^{th} lattice site. In Fig. 1.6 we show a Wannier orbital centered at the origin.

An intuitive picture of the form of a Wannier function can be gained if one assumes the periodic function $u_q^{(n)}(x)$ in equation 1.9 to be approximately the same for all Bloch states in a band. Under this approximation

$$w_n(x) \approx u^{(n)}(x)\frac{\sin(kx)}{kx}, \tag{1.13}$$

clearly showing that $w_n(x)$ looks likes $u^{(n)}(x)$ at the site center, but it spreads out with gradually decreasing oscillations. The latter are needed to ensure orthogonality.

1.2.3 Tight binding approximation

The tight-binding approximation deals with the case in which the overlap between Wannier orbitals at different sites is enough to require corrections to the picture of isolated particles but not too much as to render the picture of localized wave functions completely irrelevant. In this regime, to a very good approximation, one can only take into account overlap between Wannier orbitals in nearest neighbor sites. Furthermore, if initially the atoms are

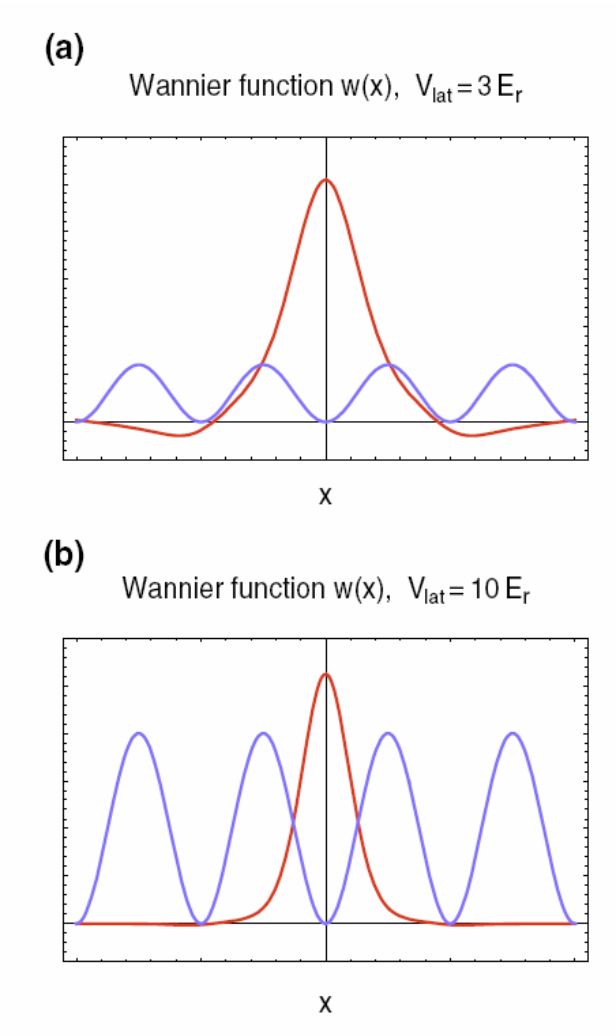

Figure 1.6 Wannier functions in a periodic potential plotted together with a schematic lattice potential. Wannier functions constitute an orthogonal set of maximally localized wave functions. For $3E_r$ side-lobes are visible, for $10E_r$ the side-lobes become very small.

prepared in the lowest band, the dynamics can be restricted to remain in the lowest band. The tight-binding model is commonly used to solve the problem of a particle in a periodic potential when also an external potential $V(x)$, not strong enough or sharp enough to induce interband transitions, is applied.

By expanding the wave function in the lowest band Wannier orbitals,

$$\Psi(x,t) = \sum_i \psi_i(t) w_0(x - x_i), \tag{1.14}$$

we get the following equations of motion

$$i\hbar \frac{\partial}{\partial t}\psi_i(t) = -J\left(\psi_{i+1}(t) + \psi_{i-1}(t)\right) + V(x_i)\psi_i(t) + \varepsilon_o \psi_i(t), \tag{1.15}$$

with

$$J = -\int dx w_0^*(x_i) H_o w_0(x - x_{i+1}) dx, \tag{1.16}$$

$$\varepsilon_o = \int dx w_0^*(x) H_o w_0(x) dx \tag{1.17}$$

J is the tunneling matrix element between nearest neighboring lattice sites which decreases exponentially with lattice depth, and ε_o is the unperturbed on site energy shift. Eq. (1.15) is known as the discrete Schrödinger equation (DSE) or tight binding Schrödinger equation.

1.2.4 Semiclassical dynamics

Formalism

Solving Eq. (1.15) is presumably not possible for an arbitrary $V(x_i)$. However, one can get general insight to the nature of solutions by the application of the correspondence principle. It is well known that wave-packet solutions of the Schrödinger equation behave like classical particles obeying the equations of motion derived from the same classical Hamiltonian. The classical Hamilton equations are

$$\dot{x} = \frac{\partial H}{\partial p}, \qquad \dot{p} = -\frac{\partial H}{\partial x}. \tag{1.18}$$

Using the resemblance of the crystal momentum or quasimomentum to the real momentum, the semiclassical equations of a wave packet in the first band of a lattice can be written as [Ashcroft and Mermin (1976), Ziman (1964)]:

$$\dot{x} = v^{(0)}(q) = \frac{1}{\hbar}\frac{dE_q^{(0)}}{dq}, \qquad \hbar\dot{q} = -\frac{dV(x)}{dx}. \tag{1.19}$$

The semiclassical equations of motion describe how the position and wave

vector of a particle evolve in the presence of an external potential entirely in terms of the band structure of the lattice. If we compare the acceleration predicted by the model with the conventional newtonian equation, $m\ddot{x} = -dV(x)/dx$, we can associate an effective mass induced by the presence of the lattice,m^*. This is given by

$$\frac{1}{m^*} = \frac{1}{\hbar^2}\frac{d^2}{dq^2}E_q^{(0)}. \tag{1.20}$$

If no external potential is applied, $V(x) = 0$, Bloch waves are the solutions of tight binding equation: $\psi_j(t) = f_j^{(q)} e^{-i(E_q t)/\hbar}$, $f_j^{(q)} = \frac{1}{\sqrt{L}} e^{iqaj}$ with L is the total number of lattice sites. If also periodic boundary conditions are assumed, the quasimomentum q is restricted to be an integer multiple of $\frac{2\pi}{La}$. The lowest energy band dispersion relation in this case is given by

$$E_q = -2J\cos(qa) \tag{1.21}$$

From the above equation it is possible to see the connection between J and the band width

$$J = \left(E_{q=\frac{\pi}{a}} - E_{q=0}\right)/4 \tag{1.22}$$

The effective mass becomes $m* = \frac{\hbar^2}{2Ja^2\cos(qa)}$ and close to the bottom of the band $q \to 0$, $m* \to \frac{\hbar^2}{2Ja^2}$. Since the tunneling decreases exponentially with the lattice depth, the effective mass grows exponentially. In the presence of interactions, the large effective mass manifests itself in a substantial enhancement of the interaction to kinetic energy ratio, in comparison to the free particle case. This is the reason why atoms in optical lattices can easily reach the strongly interaction regime. The strongly interacting regime corresponds to the regime in which the interaction energy of the atoms at a given density dominates over their characteristic quantum kinetic energy.

References

Al Khawaja, U., Andersen, J. O., Proukakis, N. P., and Stoof, H. T. C. 2002. Low dimensional Bose gases. *Physical Review A*, **66**, 013615.

Altman, E., Demler, E., and Lukin, M. D. 2004. Probing many-body states of ultracold atoms via noise correlations. *Phys. Rev. A*, **70**, 013603.

Ashcroft, N.W., and Mermin, N.D. 1976. *Solid State Physics*. Philadelphia: Saunders College.

Bakr, W. S., Peng, A., Tai, M. E., Ma, R., Simon, J., Gillen, J. I., Folling, S., Pollet, L., and Greiner, M. 2010. Probing the Superfluid-to-Mott Insulator Transition at the Single-Atom Level. *Science*, **329**, 547.

Blakie, P. B., and Porto, J. V. 2004. Adiabatic loading of bosons into optical lattices. *Phys. Rev. A*, **69**, 013603.

Bloch, I., Dalibard, J., and Zwerger, W. 2008. Many-body physics with ultracold gases. *Rev. Mod. Phys.*, **80**, 885.

Bogoliubov, N. N. 1947. On the theory of superfluidity. *J. Phys. (USSR)*, **11**, 23.

Campbell, G. K., Mun, J., Boyd, M., Medley, P., Leanhardt, A. E., Marcassa, L. G., Pritchard, D. E., and Ketterle, W. 2006. Imaging the Mott insulator shells by using atomic clock shifts. *Science*, **313**, 649.

Castin, Y., and Dum, R. 1998. Low-temperature Bose-Einstein condensates in time-dependent traps: Beyond the U(1) symmetry-breaking approach. *Physical Review A*, **57**, 3008–3021.

Chin, C., Grimm, R., Julienne, P., and Tiesinga, E. 2010. Feshbach resonances in ultracold gases. *Rev. Mod. Phys.*, **82**, 1225.

Dalfovo, Franco, Giorgini, Stefano, Pitaevskii, Lev P., and Stringari, Sandro. 1999. Theory of Bose-Einstein condensation in trapped gases. *Reviews of Modern Physics*, **71**, 463–512.

Fisher, Matthew P. A., Weichman, Peter B., Grinstein, G., and Fisher, Daniel S. 1989. Boson localization and the superfluid-insulator transition. *Physical Review B*, **40**, 546–570.

Foelling, Simon, Widera, Artur, Muller, Torben, Gerbier, Fabrice, and Bloch, Immanuel. 2006. Formation of Spatial Shell Structure in the Superfluid to Mott Insulator Transition. *Physical Review Letters*, **97**, 060403.

Gardiner, C. W. 1997. Particle-number-conserving Bogoliubov method which demonstrates the validity of the time-dependent Gross-Pitaevskii equation for a highly condensed Bose gas. *Physical Review A*, **56**, 1414–1423.

Gemelke, Nathan, Zhang, Xibo, Hung, Chen-Lung, and Chin, Cheng. 2009. In situ observation of incompressible Mott-insulating domains in ultracold atomic gases. *Nature*, **460**, 995–998.

Gerbier, F., Widera, A., Folling, S., Mandel, O., Gericke, T., and Bloch, I. 2005a. Interference pattern and visibility of a Mott insulator. *Physical Review A*, **72**.

Gerbier, F., Widera, A., Folling, S., Mandel, O., Gericke, T., and Bloch, I. 2005b. Phase coherence of an atomic Mott insulator. *Physical Review Letters*, **95**.

Ginzburg, V. L., and Landau, L. D. 1950. On the theory of superconductivity. *Zh. Eksp. Theor. Fiz.*, **20**, 1064.

Greiner, Markus. 2003. PhD thesis: Ultracold quantum gases in three-dimensional optical lattice potentials. *Dissertation in the Physics department of the Ludwig-Maximilians-Universität München.*

Hutchinson, D. A. W., Burnett, K., Dodd, R. J., Morgan, S. A., Rusch, M., Zaremba, E., Proukakis, N. P., Edwards, M., and Clark, C. W. 2000. Gapless mean-field theory of Bose-Einstein condensates. *Journal of Physics B-Atomic Molecular and Optical Physics*, **33**, 3825–3846.

Jaksch, D., Bruder, C., Cirac, J. I., Gardiner, C. W., and Zoller, P. 1998. Cold Bosonic Atoms in Optical Lattices. *Phys. Rev. Lett.*, **81**, 3108.

Jo, Gyu-Boong, Guzman, Jennie, Thomas, Claire K., Hosur, Pavan, Vishwanath, Ashvin, and Stamper-Kurn, Dan M. 2012. Ultracold Atoms in a Tunable Optical Kagome Lattice. *Physical Review Letters*, **108**, 045305.

Morgan, S. A. 2000. A gapless theory of Bose-Einstein condensation in dilute gases at finite temperature. *Journal of Physics B-Atomic Molecular and Optical Physics*, **33**, 3847–3893.

Mott, N. F. 1949. The basis of the electron theory of metals, with special reference to the transition metals. *Proceedings of the Physical Society of London Series A*, **62**, 416.

Penrose, O., and Onsage, L. 1956. Bose-Einstein Condensation and Liquid Helium. *Phys. Rev.*, **104**, 576.

Phillips, William D. 1998. Nobel Lecture: Laser cooling and trapping of neutral atoms. *Reviews of Modern Physics*, **70**, 721–741.

Rey, A. M., Burnett, K., Roth, R., Edwards, M., Williams, C. J., and Clark, C. W. 2003. Bogoliubov approach to superfluidity of atoms in an optical lattice. *Journal of Physics B-Atomic Molecular and Optical Physics*, **36**, 825.

Sachdev, S. 2011. *Quantum Phase Transitions.* Cambridge University Press.

Schellekens, M., Hoppeler, R., Perrin, A., Gomes, J. V., Boiron, D., Aspect, A., and Westbrook, C. I. 2005. Hanbury Brown Twiss effect for ultracold quantum gases. *Science*, **310**, 648–651.

Sebby-Strabley, J., Anderlini, M., Jessen, P. S., and Porto, J. V. 2006. Lattice of double wells for manipulating pairs of cold atoms. *Phys. Rev. A*, **73**, 033605.

Sherson, J. F., Weitenberg, C., Endres, M., Cheneau, M., Bloch, I., and Kuhr, S. 2010. Single-atom-resolved fluorescence imaging of an atomic Mott insulator. *Nature*, **467**, 68.

Soltan-Panahi, P., Struck, J., Hauke, P., Bick, A., Plenkers, W., Meineke, G., Becker, C., Windpassinger, P., Lewenstein, M., and Sengstock, K. 2011. Multi-component quantum gases in spin-dependent hexagonal lattices. *Nat Phys*, **7**, 434–440.

Spielman, I. B., Phillips, W. D., and Porto, J. V. 2007. Mott-insulator transition in a two-dimensional atomic Bose gas. *Phys. Rev. Lett.*, **98**, 080404.

Tarruell, Leticia, Greif, Daniel, Uehlinger, Thomas, Jotzu, Gregor, and Esslinger, Tilman. 2012. Creating, moving and merging Dirac points with a Fermi gas in a tunable honeycomb lattice. *Nature*, **483**, 302–305.

Toth, E., Rey, A. M., and Blakie, P. B. 2008. Theory of correlations between ultracold bosons released from an optical lattice. *Phys. Rev. A*, **78**, 013627.

van Oosten, D., van der Straten, P., and Stoof, H. T. C. 2001. Quantum phases in an optical lattice. *Physical Review A*, **63**, 053601.

Wirth, Georg, Olschlager, Matthias, and Hemmerich, Andreas. 2011. Evidence for orbital superfluidity in the P-band of a bipartite optical square lattice. *Nat Phys*, **7**, 147–153.

Ziman, J.M. 1964. *Principles of the Theory of Solids*. London, England: Cambridge University Press.

2

Ultracold atoms in optical lattices

2.1 The Bose-Hubbard Hamiltonian

The simplest non trivial model that describes interacting bosons in a periodic potential is the Bose-Hubbard Hamiltonian. This model has been used to describe many different systems in solid state physics, such as short correlation length superconductors, Josephson arrays, critical behavior of ^{4}He and, recently, cold atoms in optical lattices [Bloch et al. (2008)]. The Bose-Hubbard Hamiltonian exhibits a quantum phase transition from a superfluid to a Mott insulator state [Fisher et al. (1989)]. Its phase diagram has been studied analytically and numerically with many different techniques and confirmed experimentally using ultracold atomic systems in 1D, 2D and 3D lattice geometries [Bloch et al. (2008)].

The Bose-Hubbard Hamiltonian can be derived from the second quantized Hamiltonian that describes interacting bosonic atoms in an external trapping potential plus lattice. In the grand canonical ensemble and assuming the interactions are dominated by s-wave interactions (as it is the case for in ultra cold gases) this Hamiltonian is given by [Jaksch et al. (1998)]:

$$\hat{H} = \int d\mathbf{x}\hat{\Psi}^\dagger(\mathbf{x}) \left(-\frac{\hbar^2}{2m}\nabla^2 + V_{lat}(\mathbf{x}) \right) \hat{\Psi}(\mathbf{x}) + (V(\mathbf{x}) - \mu)\hat{\Psi}^\dagger(\mathbf{x})\hat{\Psi}(\mathbf{x}) + \frac{2\pi a_s \hbar^2}{m} \int d\mathbf{x}\hat{\Psi}^\dagger(\mathbf{x})\hat{\Psi}^\dagger(\mathbf{x})\hat{\Psi}(\mathbf{x})\hat{\Psi}(\mathbf{x}), \tag{2.1}$$

where $\hat{\Psi}^\dagger(\mathbf{x})$ is the bosonic field operator which creates an atom at the position $\mathbf{x}$, $V_{latt}(\mathbf{x})$ is the periodic lattice potential, $V(\mathbf{x})$ denotes any additional slowly- varying external potential that might be present (such as a harmonic confinement used to collect the atoms), a_s is the scattering length (the single parameter which characterize the low energy collisions as explained in

Chapter 3), and m the mass of an atom. μ is the chemical potential and acts as a lagrange multiplier to fix the mean number of atoms in the grand canonical ensemble.

Similar to the noninteracting situation where we used Wannier orbitals to span the single particle wave function, it is convenient to expand the field operator in terms of Wannier orbitals. Assuming that the vibrational energy splitting between bands is the largest energy scale of the problem, atoms can be loaded only in the lowest band, where they will reside under controlled conditions. Then and one can restrict the basis to include only lowest band Wannier orbitals $w_0(\mathbf{x})$,

$$\hat{\Psi}(\mathbf{x}) = \sum_j \hat{a}_j w_0(\mathbf{x} - \mathbf{x}_j), \tag{2.2}$$

Here $\hat{a}_j$ is the annihilation operator at site j which obeys bosonic canonical commutation relations (see Chapter 2). The sum is taken over the total number of lattice sites. If Eq. (2.2) is inserted in $\hat{H}$, and only tunneling processes between nearest neighbor sites are kept and the interactions are restricted to be onsite, one obtains the Bose-Hubbard Hamiltonian

$$\hat{H}_{BH} = -J \sum_{\langle \mathbf{j},\mathbf{i} \rangle} \hat{a}_i^\dagger \hat{a}_j + \frac{1}{2} U \sum_j \hat{a}_j^\dagger \hat{a}_j^\dagger a_j a_j + \sum_n (V_j - \mu) \hat{a}_j^\dagger \hat{a}_j. \tag{2.3}$$

Here the notation $\langle \mathbf{j}, \mathbf{i} \rangle$ restricts the sum to nearest-neighbors sites. J is given by Eq.(1.16) and

$$U = \frac{4\pi a_s \hbar^2}{m} \int d\mathbf{x} \left| w_0(\mathbf{x}) \right|^4, \tag{2.4}$$

$$V_j = V(\mathbf{x}_j) \tag{2.5}$$

The first term in the Hamiltonian proportional to J is a measure of the kinetic energy of the system. Next-to-nearest neighbor tunneling amplitudes are typically two orders of magnitude smaller than nearest-neighbor ones and to a good approximation they can be neglected.

The second term of Eq.2.3 accounts for interatomic interactions. The parameter U measures the strength of the repulsion of two atoms at the same lattice site. While J decreases exponentially with lattice depth V_0, the U increases as a power law, $V_0^{D/4}$, (D is the dimensionality of the lattice).

The third term in the Hamiltonian takes into account the energy offset between lattice sites due to a slow varying external potential $V(\mathbf{x})$.

2.1.1 The superfluid to Mott insulator transition

At zero temperature the physics described by the Bose-Hubbard Hamiltonian can be divided in two different regimes. The interaction dominated regime when J is much smaller than U, and the atoms behave like an insulator: the so-called Mott insulator [Mott (1949)], and the kinetic energy dominated regime, when tunneling overwhelms the repulsion and the atoms exhibit superfluid properties. The transition between the two regimes is a consequence of the competition between the kinetic energy which tries to delocalize the particles and the interaction energy which tries to localize them and penalizes multiple-occupied lattice sites.

In the superfluid regime, the kinetic energy term dominates the Hamiltonian and the system behaves as a weakly interacting Bose gas. Quantum fluctuations can be neglected and the system can be described by a macroscopic wave function. For a translationally invariant lattice the ground state consists of all atoms in the 0-quasimomentum mode.

$$|\Psi_{\mathrm{SF}}\rangle = \frac{1}{\sqrt{N!}} \left(\hat{b}_{\mathbf{0}}^{\dagger}\right)^{N} |0\rangle, \tag{2.6}$$

where N is the total number of atoms and $\hat{b}_{\mathbf{q}}^{\dagger} = \frac{1}{\sqrt{L}} \sum_j \hat{a}_j e^{\mathrm{i}\mathbf{q}\cdot\mathbf{x}_j}$ is the annihilation operator of an atom with quasimomentum $\mathbf{q}$ and L is the total number of lattice sites. Remember a is the lattice spacing.

Since the many body state is almost a product over identical single particle wave functions, the system has a macroscopic well defined phase and large number fluctuations $\sim \sqrt{N}$. The macroscopic occupation of a single mode implies that the commutator of the annihilation and creation operators in the condensate mode can be neglected with respect to the total number of atoms in the mode. Therefore, to a good approximation the field operator can be replaced by a c-number,

$$\hat{b}_{\mathbf{0}} \to \langle \hat{b}_{\mathbf{0}} \rangle \tag{2.7}$$

this approximation can be interpreted as giving to the field operator a non-zero average, $\langle \hat{b}_{\mathbf{0}} \rangle = \sqrt{N} e^{\mathrm{i}\theta}$, and thus a well defined phase to the system. Because the original Hamiltonian is invariant under a global phase transformation, the macroscopic occupation of a single mode can be linked to a spontaneous symmetry breaking [Dalfovo et al. (1999)]. The wave function associated with the condensate mode, in this case the zero quasi-momentum eigenstate $\psi_j = \sqrt{\frac{N}{L}} e^{\mathrm{i}\theta}$, is often called "condensate wave function". The one particle density matrix $\rho_{i,j}^{(1)} \equiv \langle \hat{a}_j^{\dagger} \hat{a}_i \rangle$ in this case develops off-diagonal

long range order Ginzburg and Landau (1950), meaning that spatial correlations remain finite even for very large separation between particles: $\lim_{|i-j|\to\infty} \rho^{(1)}_{i,j} \sim \lim_{|i-j|\to\infty} \psi^*_i \psi_j \to N/L$. Strictly speaking, in finite size systems with well defined number of particles, neither the concept of broken symmetry, nor the one of off-diagonal long range order can be applied [Gardiner (1997)]. However, the condensate wave function can still be determined by diagonalization of the one particle density matrix. The eigenstate with larger eigenvalue corresponds to the condensate wave function [Penrose and Onsage (1956)].

With increasing interatomic interactions, the average kinetic energy required for an atom to hop from one site to the next becomes insufficient to overcome the interaction energy cost. Atoms tend to get localize at individual lattice sites and fluctuations of the atom number at a given lattice site penalized. In this strongly interacting limit, if the number of atoms is commensurate with the number of lattice sites, the ground state of the system enters the Mott insulator phase, characterized by localized atomic wave functions and a fixed number of atoms per site [Mott (1949)].

$$|\Psi_{\rm MI}\rangle = \prod_{\mathbf{j}} \frac{1}{\sqrt{n_o!}} (\hat{a}^\dagger_j)^{n_o} |0\rangle, \tag{2.8}$$

where $n_o = N/L$ is the filling factor or mean number of particles per site. We have assumed that the number of particles is commensurate with lattice sites, i.e. that n_o is an integer.

The lowest lying excitations that conserve particle number are particle-hole excitations (adding plus removing a particle from the system) which cost energy. The Mott phase consequently is characterized by the existence of an energy gap. The gap is determined by the energy necessary to create one particle-hole pair.

2.1.2 The phase diagram

The zero temperature phase diagram [Fisher et al. (1989)] that describes the Bose-Hubbard model in a translational invariant system ($V_j = 0$) exhibits lobe-like Mott insulating phases in the J/U-μ plane, see Fig. 2.1. Each Mott lobe is characterized by having a fixed integer density. Inside the lobes the compressibility vanishes, $\partial\rho/\partial\mu = 0$, with ρ the density of the system.

The underlying physics of this phase diagram can be understood from the following considerations. Imagine we start at some point in the Mott insulating phase and increase μ while keeping J/U fixed. Then, there is going

to be a point at which the kinetic energy of adding an extra particle and letting it hop around, will balance the interaction energy cost. With an extra particle free to move around the lattice, phase coherence is recovered and the system enters the superfluid regime. Likewise, if μ is decreased starting from a point in the Mott phase, eventually it will be energetically favorable to remove one particle from the system. The extra mobile hole will induce also phase coherence and the system will condense in a superfluid state.

Since the kinetic energy of the system increases with J the width of the lobes decreases with J. The distance in the μ axis at fixed J/U between the upper and lower part of the lobe is the energy gap. At $J = 0$ the gap is just equal to U. Also at $J = 0$ the intersection point between the lobe with density $\rho = n_0$ and the one with density $\rho = n_0 + 1$ is degenerated. Because there is not energy barrier to the addition of an extra particle at this generated points, the system remain superfluid. Mott insulator phases occur only at integer filling, non-integer density contours lie entirely in the superfluid phase because there is always an extra particle that can hop without energy cost.

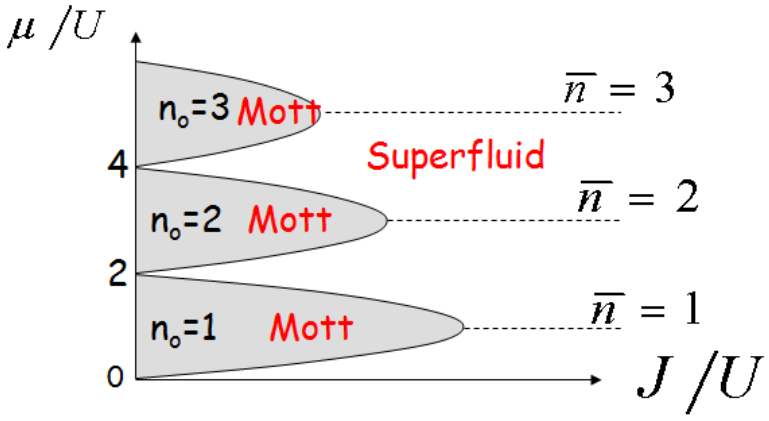

Figure 2.1 Zero temperature phase diagram of the Superfluid to Mott Insulator transition. The dashed lines are contours with fixed integer density.

The Bose-Hubbard phase diagram includes two different types of phase transitions [Fisher et al. (1989)]. One type takes place at any generic point of the phase boundary, and it is driven by the energy cost to add or subtract a particle from the incompressible Mott state as explained above. The other type, only takes place at the tip of the Mott lobes. This transition only occurs at a fixed integer density by increasing J/U and enabling the

bosons to overcome the on site repulsion. The two kinds of phase transitions belong to different universality classes [Sachdev (2011)]. In the generic one, the parameter equivalent to the reduced temperature, $\delta = T - T_c$, which describes finite temperature transitions is $\delta \sim \mu - \mu_c$, with μ_c the chemical potential at the phase boundary. For the special fixed density on the other hand one must take $\delta \sim (J/U) - (J/U)_c$, with $(J/U)_c$ the critical value at the tip the Mott lobes.

2.1.3 Decoupling mean field approximation

The Bose-Hubbard Hamiltonian is the simples model that describes interacting bosons in a lattice, however an exact analytic treatment of its phase diagram is not possible. Regardless of this difficulty, this Hamiltonian admits a simple approximated treatment, the so-called decoupling mean field approximation [Fisher et al. (1989); van Oosten et al. (2001)], that captures most of the features of the phase diagram discussed above. Here we present a brief overview of the method. The decoupling mean field approximation is carried out by introducing a real superfluid order parameter $\psi = \langle \hat{a}_\mathbf{j}^\dagger \rangle = \langle \hat{a}_j \rangle$ and then constructing a self-consistent mean-field theory. The kinetic energy term is replaced by:

$$\begin{aligned} \hat{a}_j^\dagger \hat{a}_i &\to \hat{a}_j^\dagger \langle \hat{a}_i \rangle + \langle \hat{a}_j^\dagger \rangle \hat{a}_i - \langle \hat{a}_j^\dagger \rangle \langle \hat{a}_i \rangle \\ &= \psi(\hat{a}_j^\dagger + \hat{a}_i) - \psi^2, \end{aligned} \tag{2.9}$$

when substituted into Eq. 2.3 yields

$$\hat{H}_{mean} = -Jz\psi \sum_j (\hat{a}_j^\dagger + \hat{a}_j - \psi) + \frac{1}{2} U \sum_j \hat{a}_j^\dagger \hat{a}_j^\dagger a_j a_j + \sum_j (-\mu) \hat{a}_j^\dagger \hat{a}_j \tag{2.10}$$

Here $z = 2D$ is the number of nearest-neighbor sites and L is the total number of lattice sites. This Hamiltonian is local and the same for each lattice site, therefore we will drop the subscript j in the following discussion.

By treating ψ as a small parameter, one can use perturbation theory to calculate the mean field energy. Assuming commensurate filling $N/L = n_0 = 1, 2, \ldots$, to zero order in ψ the ground state of the system will have energy $E_{n_0}^{(0)}$ and exactly n_0 particles per site (Eq.3.37). In this unperturbed occupation number basis the odd powers of the expansion of the energy in ψ will always be zero. Up to four order, the ground state energy becomes

$$E = E^{(0)} + \psi^2 E^{(2)} + \psi^4 E^{(4)} \tag{2.11}$$

with $E^{(2)} = \sum_{m=-1,m\neq 0}^{1} \frac{|\langle n_0|Jz(\hat{a}+\hat{a}^\dagger)|n_0+m\rangle|^2}{E^{(0)}_{n_0}-E^{(0)}_{n_0+m}} + Jz$. If we now minimize the energy as a function of ψ, we find that $\psi \neq 0$ when $E^{(2)} < 0$ and that $\psi = 0$ when $E^{(2)} > 0$. This means that $E^{(2)} = 0$ determines the boundary between the superfluid and the insulator phases. The solution $E^{(2)} = 0$ occurs for [van Oosten et al. (2001)]

$$\frac{\mu^{\pm}}{Jz} = \frac{1}{2}\left(\frac{U}{Jz}(2n_0-1) - 1 \pm \sqrt{\left(\frac{U}{Jz}\right)^2 - 2\frac{U}{Jz}(2n_0+1)+1}\right) \tag{2.12}$$

By equating $\mu^+ = \mu^-$ one finds the critical value at the tip of each lobe:

$$\left(\frac{U}{J}\right)_c = z\left(2n_0 + 1 + \sqrt{(2n_0+1)^2 - 1}\right) \tag{2.13}$$

2.1.4 Bogoliubov treatment of the superfluid to Mott transition

An alternative systematic approach to deal with the weakly interacting regime of the Bose-Hubbard model uses the ideas developed by N. Bogoliubov in 1947 [Bogoliubov (1947)]. The Bogoliubov approximation treats the field operator as a c-number plus a small fluctuating term. The c-number describes the condensate or the coherent part of the bosonic matter field and the fluctuating term accounts for quantum correlations. Since in a weakly interacting gas quantum correlations are small, one can neglect third and higher order terms in the fluctuating field and derive an effective quadratic Hamiltonian which can be exactly diagonalized. In the following, we will apply the Bogoliubov approximation to the Bose-Hubbard Hamiltonian and derive the correspondent Bogoliubov-de Genes(BdG) equations as developed in Refs. [van Oosten et al. (2001); Rey et al. (2003)]. We will restrict our analysis to $T = 0$.

The Bogoliubov approximation

In the very weakly interacting regime, to a good approximation, the field operator can be written in terms of a *c*-number plus a fluctuation operator:

$$\hat{a}_j = \psi_j + \hat{\varphi}_j. \tag{2.14}$$

Replacing this expression for $\hat{a}_j$ in the Bose-Hubbard Hamiltonian leads to :

$$\hat{H} = E_o + \hat{H}_1 + \hat{H}_2 + \hat{H}_3 + \hat{H}_4, \tag{2.15}$$

with

$$H_0 = -J \sum_{\langle i,j \rangle} \psi_i^* \psi_j + \sum_i (V_i - \mu)|\psi_i|^2 + \frac{U}{2}|\psi_i|^4, \tag{2.16}$$

$$\hat{H}_1 = -J \sum_{\langle i,j \rangle} \hat{\varphi}_i \psi_j^* + \sum_i \left(V_i - \mu + U|\psi_i|^2\right) \psi_i^* \hat{\varphi}_i + h.c., \tag{2.17}$$

$$\hat{H}_2 = -J \sum_{\langle i,j \rangle} \hat{\varphi}_i^\dagger \hat{\varphi}_j + \sum_i (V_i - \mu) \hat{\varphi}_i^\dagger \hat{\varphi}_i + \frac{U}{2} \sum_i \left(\hat{\varphi}_i^{2\dagger} \psi_i^2 + \hat{\varphi}_i^2 \psi_i^{2*} + (\hat{\varphi}_i^\dagger \hat{\varphi}_i + \hat{\varphi}_i \hat{\varphi}_i^\dagger)|\psi_i|^2 \right), \tag{2.18}$$

$$\hat{H}_3 = U \sum_i \hat{\varphi}_i^\dagger \hat{\varphi}_i^\dagger \hat{\varphi}_i \psi_i + h.c., \tag{2.19}$$

$$\hat{H}_4 = \frac{U}{2} \sum_i \hat{\varphi}_i^\dagger \hat{\varphi}_i^\dagger \hat{\varphi}_i \hat{\varphi}_i, \tag{2.20}$$

where $\langle i, j \rangle$ restricts the sum over nearest neighbors and *h.c.* stands for the hermitian adjoint. The terms of the Hamiltonian have been grouped in equations according to the number of non-condensate operators which they contain.

The first step is the minimization of the energy functional H_0. This requires the condensate amplitudes ψ_i to be a solution of the following nonlinear equation,

$$\mu \psi_i = -J \sum_{\langle i,j \rangle} \psi_j + (V_i + U|\psi_i|^2)\psi_i \tag{2.21}$$

This equation is known as the discrete nonlinear Schrödinger equation (DNLSE). It is a discrete version of the Gross-Pitaevskii equation (GPE) (See Chapter 3). It can be also obtained by expanding the GPE equation in a Wannier orbital basis and then using the tight binding approximation (see Sec1.15). When ψ_i is a solution of Eq.2.21 the linear Hamiltonian $\hat{H}_1$ vanishes.

The quadratic Hamiltonian $\hat{H}_2$ accounts for the leading order corrections to the DNLSE due to quantum fluctuations. The basis that diagonalizes $\hat{H}_2$ defines the so -called quasiparticle states. Mathematically the diagonalization procedure involves a linear canonical transformation of the single-particle creation and annihilation operators $\hat{a}_i^\dagger$ and $\hat{a}_i$ into quasiparticle op-

erators $\hat{\alpha}^{\dagger}_{\mathbf{s}}$,$\hat{\alpha}_{\mathbf{s}}$. This transformation is what is known as Bogoliubov transformation and is given by

$$\hat{\varphi}_i = \sum_{\mathbf{s}\neq 0} u_i^{\mathbf{s}} \hat{\alpha}_{\mathbf{s}} - v_i^{*\mathbf{s}} \hat{\alpha}^{\dagger}_{\mathbf{s}}. \tag{2.22}$$

In general the spectrum of fluctuations includes a zero mode $\mathbf{s} = 0$. This mode is the Goldstone boson associated with the breaking of global phase invariance by the condensate. The zero mode is essentially non-perturbative and it introduces an artificial infrared divergence in low dimensional models. For this reason quadratic approximations are actually improved if the contribution from this mode is neglected all together [Al Khawaja et al. (2002)]. A different way to deal with the zero mode has been proposed by Castin and Dum (1998); Gardiner (1997); Hutchinson et al. (2000); Morgan (2000). For simplicity we are going to ignore zero mode fluctuations and restrict the fluctuation operators to act only on the excited states.

The Bogoliubov transformation Eq. 2.22 is required to be canonical. By canonical it is meant that it preserves the commutation relations and leads to bosonic quasiparticles. To satisfy it, the amplitudes $\{u_i^{\mathbf{s}}, v_i^{\mathbf{s}}\}$ are constrained by the conditions:

$$\sum_i u_i^{*\mathbf{s}} u_i^{\mathbf{s}\prime} - v_i^{*\mathbf{s}} v_i^{\mathbf{s}\prime} = \delta_{\mathbf{s}\mathbf{s}\prime}, \tag{2.23}$$

$$\sum_{\mathbf{i}} u_i^{\mathbf{s}} v_i^{\mathbf{s}\prime} - v_i^{*\mathbf{s}} u_i^{*\mathbf{s}\prime} = 0. \tag{2.24}$$

The necessary and sufficient conditions that the quasiparticle amplitudes have to fulfill to diagonalize the Hamiltonian are provided by the so called Bogoliubov-de Gennes (BdG) equations

$$\begin{pmatrix} \mathcal{L} & \mathcal{M} \\ \mathcal{M}^* & \mathcal{L} \end{pmatrix} \begin{pmatrix} \mathbf{u}^{\mathbf{s}} \\ \mathbf{v}^{\mathbf{s}} \end{pmatrix} = \omega_s^B \begin{pmatrix} \mathbf{u}^{\mathbf{s}} \\ -\mathbf{v}^{\mathbf{s}} \end{pmatrix} \tag{2.25}$$

with $\mathbf{u}^{\mathbf{s}} = (u_1^{\mathbf{s}}, u_2^{\mathbf{s}} \dots u_L^{\mathbf{s}})$, $\mathbf{v}^{\mathbf{s}} = (v_1^{\mathbf{s}}, v_2^{\mathbf{s}} \dots v_L^{\mathbf{s}})$ and $\boldsymbol{\psi} = (\psi_1, \psi_2 \dots \psi_L)$. The matrices $\mathcal{L}$ and $\mathcal{M}$ are given by

$$\mathcal{L}_{ij} = -Jf(i,j) + \delta_{ij}(2U|\psi_i|^2 + V_i - \mu) \tag{2.26}$$

$$\mathcal{M}_{ij} = -U\psi_i^2 \delta_{ij}. \tag{2.27}$$

with δ_{ij} the Kronecker delta which is one if $i = j$ and zero otherwise and $f(i,j)$ a function which is equal to one if the sites i and j are nearest-neighbors and zero otherwise. If the BdG equations are satisfied, the quadratic Hamiltonian, up to constant terms, takes the form

$$\hat{H}_2 = \sum_{\mathbf{s}\neq 0} \omega_{\mathbf{s}}^B \hat{\alpha}_{\mathbf{s}}^\dagger \hat{\alpha}_{\mathbf{s}}. \tag{2.28}$$

The quasi-particle energies $\omega_{\mathbf{s}}^B$ come in pairs: if $\omega_{\mathbf{s}}^B$is a solution for the amplitudes $(\mathbf{u}^{\mathbf{s}}, \mathbf{v}^{\mathbf{s}})$ then $-\omega_{\mathbf{s}}^B$is also a solution for the amplitudes $(\mathbf{v}^{\mathbf{s}*}, \mathbf{u}^{\mathbf{s}*})$. The solution with zero energy is always a solution and in this case the amplitudes must be proportional to the condensate $(\mathbf{v}^{\mathbf{0}}, \mathbf{u}^{\mathbf{0}}) \propto (\boldsymbol{\psi}, \boldsymbol{\psi})$. We explicitly exclude the zero mode solution to guarantee that the excitations are orthogonal to the condensate.

In a zero temperature gas the fraction of atoms which are not part of the condensate is generally referred to as the quantum depletion, ρ_d, Under the Bogoliubov approximation, the quantum depletion is given by

$$\rho_d = \sum_j \left\langle \hat{\varphi}_j^\dagger \hat{\varphi}_j \right\rangle = \sum_{j,\mathbf{s}\neq 0} |v_j^{\mathbf{s}}|^2 \tag{2.29}$$

$$N = \sum_j |\psi_j|^2 + \rho_d \tag{2.30}$$

Translationally invariant system

To understand the physics captured by the Bogoliubov approximation, we study the case where no external confinement is present, $V_j = 0$. We assume a D dimensional separable square optical lattice with equal tunneling matrix element J in all directions and periodic boundary conditions. The total number of sites is again L.

Due to the translational symmetry of the system the condensate amplitudes are constant over the lattice, $\psi_j = \sqrt{n_c}$. The quasiparticle modes have a plane wave character and therefore can be related to quasimomentum modes:

$$u_j^{\mathbf{q}} = \frac{1}{\sqrt{L}} e^{i\mathbf{q}\cdot\mathbf{x}_j} u_{\mathbf{q}}, \quad v_j^{\mathbf{q}} = \frac{1}{\sqrt{L}} e^{i\mathbf{q}\cdot\mathbf{x}_j} v_{\mathbf{q}}. \tag{2.31}$$

Here the vector $\mathbf{q} = \{q_1, q_2, \ldots q_d\}$ denotes the quasi-momentum, whose components assume discrete values which are integer multiples of $\frac{2\pi}{a\sqrt[D]{L}}$. a is the lattice spacing. The amplitudes $u_{\mathbf{q}}$ and $v_{\mathbf{q}}$ must satisfy the condition $|u_{\mathbf{q}}|^2 - |v_{\mathbf{q}}|^2 = 1$ and can all be chosen to be real and to depend only on the modulus of the wave vector ($u_{\mathbf{q}} = u_{-\mathbf{q}}$, $v_{\mathbf{q}} = v_{-\mathbf{q}}$).

In the translationally invariant system the DNLSE reduces to

$$\mu = -zJ + n_c U \tag{2.32}$$

where z is the number of nearest neighbors $z = 2D$.

The BdG equations become the following 2×2 eigenvalue problem

$$\begin{pmatrix} \mathcal{L}_{\mathbf{qq}} & -\mathcal{M}_{\mathbf{q-q}} \\ \mathcal{M}_{\mathbf{q-q}} & -\mathcal{L}_{\mathbf{qq}} \end{pmatrix} \begin{pmatrix} u_{\mathbf{q}} \\ v_{\mathbf{q}} \end{pmatrix} = \omega_{\mathbf{q}} \begin{pmatrix} u_{\mathbf{q}} \\ v_{\mathbf{q}} \end{pmatrix}, \tag{2.33}$$

with

$$\mathcal{L}_{\mathbf{qq}} = \epsilon_{\mathbf{q}} + n_c U, \quad \mathcal{M}_{\mathbf{q-q}} = n_c U. \tag{2.34}$$

Here we have introduced the definition $\epsilon_{\mathbf{q}} = 4J \sum_{i=1}^{D} \sin^2(\frac{q_i a}{2})$.

The quasiparticle energies $\omega_{\mathbf{q}}$ and modes are found by diagonalizing Eq.(2.34):

$$\omega_{\mathbf{q}}^2 = \mathcal{L}_{\mathbf{qq}}^2 - \mathcal{M}_{\mathbf{q-q}}^2 = {\epsilon_{\mathbf{q}}}^2 + 2U n_c \epsilon_{\mathbf{q}}, \tag{2.35}$$

$$u_{\mathbf{q}}^2 = \frac{\mathcal{L}_{\mathbf{qq}} + \omega_{\mathbf{q}}}{2\omega_{\mathbf{q}}} = \frac{\epsilon_{\mathbf{q}} + n_c U + \omega_{\mathbf{q}}}{2\omega_{\mathbf{q}}}, \tag{2.36}$$

$$v_{\mathbf{q}}^2 = \frac{\mathcal{L}_{\mathbf{qq}} - \omega_{\mathbf{q}}}{2\omega_{\mathbf{q}}} = \frac{\epsilon_{\mathbf{q}} + n_c U - \omega_{\mathbf{q}}}{2\omega_{\mathbf{q}}}, \tag{2.37}$$

$$u_{\mathbf{q}} v_{\mathbf{q}} = -\frac{\mathcal{M}_{\mathbf{q-q}}}{2\omega_{\mathbf{q}}} = \frac{n_c U}{2\omega_{\mathbf{q}}} \tag{2.38}$$

and

$$n = n_c + \frac{1}{L} \sum_{\mathbf{q} \neq \mathbf{0}} v_{\mathbf{q}}^2, \tag{2.39}$$

with n the total density, $n = N/L$. The constrain that fixes the number of particles can be written as

$$n_c = n - \frac{1}{L} \sum_{\mathbf{q} \neq \mathbf{0}} \left(\frac{\epsilon_{\mathbf{q}} + U n_c}{2\omega_{\mathbf{q}}} - \frac{1}{2} \right). \tag{2.40}$$

Note that, as opposed to the free particle system where for high momentum always the single particle energy (which grows as q^2) is dominant, in the presence of the lattice the single particle excitations are always bounded by $4JD$, when the atoms are restricted to populate the first band. Therefore, in the regime $Un_c/J > 1$ the interaction term dominates for all quasimomentum and so $\omega_{\mathbf{q}} \sim \sqrt{2Un_c\epsilon_{\mathbf{q}}}$. Thus, to a good approximation the condensate fraction can be written as:

$$n_c \approx g - \sqrt{\frac{Un_c}{J}}\alpha \tag{2.41}$$

with

$$\alpha = \alpha(D, L) \equiv \frac{1}{L} \sum_{\mathbf{q} \neq \mathbf{0}} \frac{\sqrt{J}}{2\sqrt{2\epsilon_{\mathbf{q}}}} \tag{2.42}$$

$$g = n + \frac{L-1}{2L} \tag{2.43}$$

α is a dimensionless quantity which depends only on the dimensionality of the system and L. Because Eqs. ((2.35)-(2.36)) are completely determined if n_c is known, by solving Eq. (2.41) we obtain all necessary information. The solution of the algebraic equation is:

$$n_c \approx g + \frac{\alpha^2 U}{2J} - \sqrt{g\frac{\alpha^2 U}{J} + \frac{\alpha^4 U^2}{4J^2}}. \tag{2.44}$$

Eq. (2.44) tells us that in the strongly interacting regime the condensate fraction decreases with increasing U/J but it only vanishes when $U/J \to \infty$. The BdG equations therefore fail to predict any superfluid to Mott insulator phase transition. Since for non-integer fillings the system is never a Mott insulator, the BdG equations describe much better the incommensurate regime.

2.1.5 External trapping potential

Up to this point we have discussed the basic aspects of the superfluid-Mott insulator transition in a translationally invariant system. The situation is different for a inhomogeneous system with a fixed total number of atoms and external confinement. This is the case realized in experiments, where besides the lattice there is a harmonic trap that collects the atoms at the center. In this case, the density of atoms is not fixed since the atoms can redistribute over the lattice and change the local filling factor.

To deal with the inhomogeneous case, it is possible to define an effective local chemical potential, $\mu_{\mathbf{j}} = \mu - V_{\mathbf{j}}$, at each lattice site $\mathbf{j}$. If the change in the mean number of atoms between neighboring sites is small, the system can be treated locally as an homogeneous system. Because in the inhomogeneous case, the local chemical potential is fixed by the density, as the ratio U/J is changed the system can cross locally the boundary between the superfluid and Mott insulator phases. For example if the chemical potential at the trap center falls into the $n_0 = 2$ Mott lobe, one obtains a series of Mott domains separated by a superfluid as one moves from the enter to the edge

of the cloud. In this manner, all different phases that exist for given J/U are present simultaneously.

The existence of such "wedding-cake-like" density profiles in the Mott insulator regime is supported by Monte Carlo calculations in one, two, and three dimensions [Bloch et al. (2008)]. The shell structure has been experimentally measured by using indirect methods such as mean field shifts [Campbell et al. (2006)] and spatially selective microwave transitions together with spin changing collisions [Foelling et al. (2006)]. Just recently direct in-situ imaging methods with single lattice site resolution have successfully resolved the shell structure in 2D systems [Gemelke et al. (2009); Bakr et al. (2010); Sherson et al. (2010)].

References

Al Khawaja, U., Andersen, J. O., Proukakis, N. P., and Stoof, H. T. C. 2002. Low dimensional Bose gases. *Physical Review A*, **66**, 013615.

Altman, E., Demler, E., and Lukin, M. D. 2004. Probing many-body states of ultracold atoms via noise correlations. *Phys. Rev. A*, **70**, 013603.

Ashcroft, N.W., and Mermin, N.D. 1976. *Solid State Physics*. Philadelphia: Saunders College.

Bakr, W. S., Peng, A., Tai, M. E., Ma, R., Simon, J., Gillen, J. I., Folling, S., Pollet, L., and Greiner, M. 2010. Probing the Superfluid-to-Mott Insulator Transition at the Single-Atom Level. *Science*, **329**, 547.

Blakie, P. B., and Porto, J. V. 2004. Adiabatic loading of bosons into optical lattices. *Phys. Rev. A*, **69**, 013603.

Bloch, I., Dalibard, J., and Zwerger, W. 2008. Many-body physics with ultracold gases. *Rev. Mod. Phys.*, **80**, 885.

Bogoliubov, N. N. 1947. On the theory of superfluidity. *J. Phys. (USSR)*, **11**, 23.

Campbell, G. K., Mun, J., Boyd, M., Medley, P., Leanhardt, A. E., Marcassa, L. G., Pritchard, D. E., and Ketterle, W. 2006. Imaging the Mott insulator shells by using atomic clock shifts. *Science*, **313**, 649.

Castin, Y., and Dum, R. 1998. Low-temperature Bose-Einstein condensates in time-dependent traps: Beyond the U(1) symmetry-breaking approach. *Physical Review A*, **57**, 3008–3021.

Chin, C., Grimm, R., Julienne, P., and Tiesinga, E. 2010. Feshbach resonances in ultracold gases. *Rev. Mod. Phys.*, **82**, 1225.

Dalfovo, Franco, Giorgini, Stefano, Pitaevskii, Lev P., and Stringari, Sandro. 1999. Theory of Bose-Einstein condensation in trapped gases. *Reviews of Modern Physics*, **71**, 463–512.

Fisher, Matthew P. A., Weichman, Peter B., Grinstein, G., and Fisher, Daniel S. 1989. Boson localization and the superfluid-insulator transition. *Physical Review B*, **40**, 546–570.

Foelling, Simon, Widera, Artur, Muller, Torben, Gerbier, Fabrice, and Bloch, Immanuel. 2006. Formation of Spatial Shell Structure in the Superfluid to Mott Insulator Transition. *Physical Review Letters*, **97**, 060403.

Gardiner, C. W. 1997. Particle-number-conserving Bogoliubov method which demonstrates the validity of the time-dependent Gross-Pitaevskii equation for a highly condensed Bose gas. *Physical Review A*, **56**, 1414–1423.

Gemelke, Nathan, Zhang, Xibo, Hung, Chen-Lung, and Chin, Cheng. 2009. In situ observation of incompressible Mott-insulating domains in ultracold atomic gases. *Nature*, **460**, 995–998.

Gerbier, F., Widera, A., Folling, S., Mandel, O., Gericke, T., and Bloch, I. 2005a. Interference pattern and visibility of a Mott insulator. *Physical Review A*, **72**.

Gerbier, F., Widera, A., Folling, S., Mandel, O., Gericke, T., and Bloch, I. 2005b. Phase coherence of an atomic Mott insulator. *Physical Review Letters*, **95**.

Ginzburg, V. L., and Landau, L. D. 1950. On the theory of superconductivity. *Zh. Eksp. Theor. Fiz.*, **20**, 1064.

Greiner, Markus. 2003. PhD thesis: Ultracold quantum gases in three-dimensional optical lattice potentials. *Dissertation in the Physics department of the Ludwig-Maximilians-Universität München.*

Hutchinson, D. A. W., Burnett, K., Dodd, R. J., Morgan, S. A., Rusch, M., Zaremba, E., Proukakis, N. P., Edwards, M., and Clark, C. W. 2000. Gapless mean-field theory of Bose-Einstein condensates. *Journal of Physics B-Atomic Molecular and Optical Physics*, **33**, 3825–3846.

Jaksch, D., Bruder, C., Cirac, J. I., Gardiner, C. W., and Zoller, P. 1998. Cold Bosonic Atoms in Optical Lattices. *Phys. Rev. Lett.*, **81**, 3108.

Jo, Gyu-Boong, Guzman, Jennie, Thomas, Claire K., Hosur, Pavan, Vishwanath, Ashvin, and Stamper-Kurn, Dan M. 2012. Ultracold Atoms in a Tunable Optical Kagome Lattice. *Physical Review Letters*, **108**, 045305.

Morgan, S. A. 2000. A gapless theory of Bose-Einstein condensation in dilute gases at finite temperature. *Journal of Physics B-Atomic Molecular and Optical Physics*, **33**, 3847–3893.

Mott, N. F. 1949. The basis of the electron theory of metals, with special reference to the transition metals. *Proceedings of the Physical Society of London Series A*, **62**, 416.

Penrose, O., and Onsage, L. 1956. Bose-Einstein Condensation and Liquid Helium. *Phys. Rev.*, **104**, 576.

Phillips, William D. 1998. Nobel Lecture: Laser cooling and trapping of neutral atoms. *Reviews of Modern Physics*, **70**, 721–741.

Rey, A. M., Burnett, K., Roth, R., Edwards, M., Williams, C. J., and Clark, C. W. 2003. Bogoliubov approach to superfluidity of atoms in an optical lattice. *Journal of Physics B-Atomic Molecular and Optical Physics*, **36**, 825.

Sachdev, S. 2011. *Quantum Phase Transitions.* Cambridge University Press.

Schellekens, M., Hoppeler, R., Perrin, A., Gomes, J. V., Boiron, D., Aspect, A., and Westbrook, C. I. 2005. Hanbury Brown Twiss effect for ultracold quantum gases. *Science*, **310**, 648–651.

Sebby-Strabley, J., Anderlini, M., Jessen, P. S., and Porto, J. V. 2006. Lattice of double wells for manipulating pairs of cold atoms. *Phys. Rev. A*, **73**, 033605.

Sherson, J. F., Weitenberg, C., Endres, M., Cheneau, M., Bloch, I., and Kuhr, S. 2010. Single-atom-resolved fluorescence imaging of an atomic Mott insulator. *Nature*, **467**, 68.

Soltan-Panahi, P., Struck, J., Hauke, P., Bick, A., Plenkers, W., Meineke, G., Becker, C., Windpassinger, P., Lewenstein, M., and Sengstock, K. 2011. Multi-component quantum gases in spin-dependent hexagonal lattices. *Nat Phys*, **7**, 434–440.

Spielman, I. B., Phillips, W. D., and Porto, J. V. 2007. Mott-insulator transition in a two-dimensional atomic Bose gas. *Phys. Rev. Lett.*, **98**, 080404.

Tarruell, Leticia, Greif, Daniel, Uehlinger, Thomas, Jotzu, Gregor, and Esslinger, Tilman. 2012. Creating, moving and merging Dirac points with a Fermi gas in a tunable honeycomb lattice. *Nature*, **483**, 302–305.

Toth, E., Rey, A. M., and Blakie, P. B. 2008. Theory of correlations between ultracold bosons released from an optical lattice. *Phys. Rev. A*, **78**, 013627.

van Oosten, D., van der Straten, P., and Stoof, H. T. C. 2001. Quantum phases in an optical lattice. *Physical Review A*, **63**, 053601.

Wirth, Georg, Olschlager, Matthias, and Hemmerich, Andreas. 2011. Evidence for orbital superfluidity in the P-band of a bipartite optical square lattice. *Nat Phys*, **7**, 147–153.

Ziman, J.M. 1964. *Principles of the Theory of Solids*. London, England: Cambridge University Press.